Ludden, J.N., Plank, T., and Escutia, C. (Eds.)
Proceedings of the Ocean Drilling Program, Scientific Results Volume 185

8. Correlation Between Core, Logging, and Seismic Data at Site 1149 in the Nadezhda Basin[1]

Lewis J. Abrams[2]

F1. Predicted topography of the northwest Pacific, p. 10.

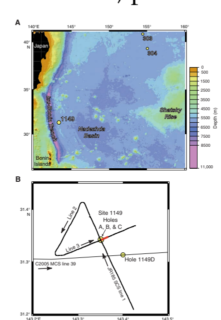

ABSTRACT

Synthetic seismograms are derived from a combination of laboratory and downhole measurements of density and velocity data collected from Holes 1149A and 1149B during Ocean Drilling Program Leg 185. The close match between single-channel seismic data obtained at Site 1149 and the synthetic seismogram facilitates core depth to traveltime correlation and is used to adjust laboratory measurements of velocity to in situ values. The two most prominent reflections are shown to correspond to the interface between pelagic clay and shallowest chert and to the top of oceanic crust. The correlation of physical and seismic stratigraphy at Site 1149 forms the basis for future regional-scale investigations of the sedimentary and volcanic history of the Nadezhda Basin, northwest Pacific.

INTRODUCTION

Ocean Drilling Program (ODP) Site 1149 is located on the Pacific plate ~100 km east of the Izu-Bonin Trench within the region known as the Nadezhda Basin (Fig. F1A). The primary objective of drilling at this site was to determine the geochemical input to the Izu-Bonin subduction system (Shipboard Scientific Party, 2000b). Site 1149 is particularly important because no other drilling attempts within 1000 km have continuously cored the entire sedimentary sequence and uppermost oceanic crust, the most proximal being Deep Sea Drilling Project (DSDP) Sites 303 and 304, 1600 km to the northeast (Fig. F1A). Single-

[1]Abrams, L.J., 2002. Correlation between core, logging, and seismic data at Site 1149 in the Nadezhda Basin. *In* Ludden, J.N., Plank, T., and Escutia, C. (Eds.), *Proc. ODP, Sci. Results,* 185, 1–14 [Online]. Available from World Wide Web: <http://www-odp.tamu.edu/publications/185_SR/VOLUME/CHAPTERS/001.PDF>. [Cited YYYY-MM-DD]
[2]University of North Carolina, Center for Marine Science, One Marvin Moss Lane, Wilmington NC 28409, USA. **abramsl@uncwil.edu**

Initial receipt: 28 August 2001
Acceptance: 31 May 2002
Web publication: 6 September 2002
Ms 185SR-001

channel seismic (SCS) profiles obtained across Site 1149 during Leg 185 and numerous regional seismic profiles throughout the area provide the means for extending the results from Site 1149 to basinwide scales (1000 km). Such regional-scale seismic stratigraphy forms the foundation for investigations of the sedimentary and volcanic history of a significant area of the northwest Pacific seaward of the Izu-Bonin Trench. The objective of this paper is to provide the correlation between the physical stratigraphy at Site 1149 and local SCS data utilizing a synthetic seismogram constructed from both downhole logging and shipboard physical properties data.

DATA

Seismic Data

Site selection for Site 1149 was initially based on multichannel seismic (MCS) lines and sonobuoy data obtained during cruise C2005 of the *Robert Conrad* in 1976. A short SCS and 3.5-kHz survey was conducted on approach to Site 1149, which confirmed the general seismic character and unit thicknesses observed in the MCS records. Holes 1149A, 1149B, and 1149C are located at the intersection of *JOIDES Resolution* SCS lines 1 and 3, which is ~3.5 km northwest of the intersection of SCS line 1 and C2005 line 39 (Fig. **F1B**). Hole 1149D is located ~5 km to the southwest on C2005 line 39. Approximately 50 km of SCS data were shot with two synchronized 80-in^3 water guns and received using a single-channel 100-m-long streamer. The guns and streamer were both towed at 12–18 m depth. Water guns were fired every 13 s, equivalent to ~36 m at 5.4 kt. The seismic data from each shot were sampled every 1 ms from 0 to 11 s and were digitally recorded after applying an antialiasing filter with a corner frequency at 250 Hz.

Site 1149 Core Data

Depth in meters below seafloor (mbsf), lithology, lithologic unit divisions, and biostratigraphic ages from Holes 1149A and 1149B (Shipboard Scientific Party, 2000c) are summarized in Figure **F2.** Results from Holes 1149C and 1149D are not considered in this study because cores were washed and/or taken discontinuously through most of the sediment section and downhole measurements were not obtained.

F2. Logging and coring results and core-log-seismic correlation, p. 11.

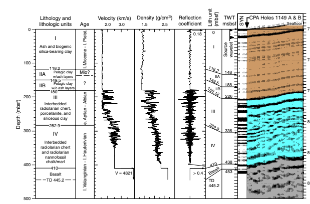

Physical Properties

The wet bulk density of discrete samples was obtained during routine measurements of index properties at Site 1149 during Leg 185 (Shipboard Scientific Party, 2000c, 2000a). Laboratory *P*-wave measurements used in this study were made using the Hamilton Frame velocimeter PWS3 contact probe system (Boyce, 1976; Blum, 1997). The PWS3 measurement is conducted across the split core axis (x-direction) using vertically oriented transducer pairs, with the upper transducer pressed against the split surface and the lower pressed against the core liner. Velocities were also measured in three mutually perpendicular directions (x, y, and z) using the PWS3 system on discrete samples of igneous and sedimentary rocks (lithologic Units III and IV and oceanic crust), which were sawed as oriented cubes. Velocity and density values were obtained every 1.5 m at the same depth in Unit I and Subunit IIA where core recovery was ~95%; however, wet bulk density values for an ~30-m interval in Subunit IIB could not be obtained because the pyncnometer did not attain a stable helium pressure (Shipboard Scientific Party, 2000c).

Downhole Measurements Data

Downhole measurements of velocity were made every 0.15 m in Hole 1149B using the long-spacing sonic sonde (LSS) as part of the combination of instruments (tools) known as the Formation MicroScanner-sonic tool string. The LSS consists of two transmitters spaced 0.61 m apart, which are located 2.4 m below two receivers that are also spaced 0.61 m apart. Velocity is calculated from measured traveltime between transmitter/receiver pairs over a known distance (i.e., 2.4, 3, 3, and 3.6 m), resulting in a maximum of four traveltime values at each measurement depth. During postcruise processing, all traveltimes resulting in velocities outside the range of 1524–3805 m/s were discarded (Lamont-Doherty Borehole Research Group). This simple reprocessing successfully corrects most noisy data because the inaccurate traveltimes are sufficiently extreme and there is an eightfold redundancy of measurements at each depth. The velocity values used in this study (known as V_{P2}) were derived from the median values of the processed traveltimes.

Downhole density measurements were made in Hole 1149B with the Hostile Environment Litho-Density Sonde (HLDS) located in the middle of the 30-m-long triple combination tool string. The HLDS utilizes an eccentralizing arm to maintain sensor contact with the borehole wall to a maximum hole diameter of 46 cm. Data accuracy is degraded by washouts where borehole diameter exceeds 46 cm. Density values above 180 mbsf within the pelagic clay are considered unreliable and are not used in this study because of extended washout zones (Fig. F3).

F3. Lithology and lithologic units and downhole measurements, p. 12.

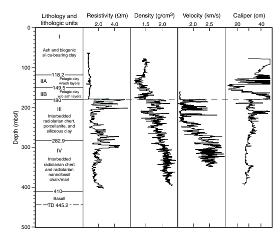

Combined Core and Logging Data

Velocity and density data used to calculate synthetic seismograms were obtained from combining laboratory and downhole logging measurements. Downhole tools record continuous measurements of in situ borehole properties, regardless of core recovery, at a relatively fine sampling interval of ~15 cm. Downhole measurements are used where possible and are especially valuable in intervals of low core recovery (e.g., below 180 mbsf). Laboratory measurements were used in discrete depth intervals where downhole measurements were either not available or were considered unreliable. Core and logging depth scales match exactly at the lithologic Unit II/III boundary (~180 mbsf), and depths reported for all major lithologic unit boundaries are from core depths.

In Hole 1149A, there was nearly 95% core recovery using the advanced hydraulic piston corer (APC) and extended core barrel (XCB) to the base of the pelagic clay interval at 180 mbsf (lithologic Units I and II) (Fig. F2). Downhole measurements of density and velocity were very limited in this interval (poor quality and/or minimal coverage) (Fig. F3); therefore, laboratory velocity and density values from Hole 1149A are used from 0 to 180 mbsf. A constant density of 1.36 g/cm^3, which is the density value measured at the top of Subunit IIB, was also used for the lower portion of this unit from 149 to 180 mbsf. Laboratory measurements can accurately reflect actual velocity and density trends in such intervals of high recovery, minimal core disturbance (i.e., APC), and relatively frequent sampling (every 1.5 m). Core recovery, however, dropped dramatically to ~10%–15% when using a rotary core barrel (RCB) in the interval of interbedded chert/porcellanite/clay and chert/chalk/marl, characterizing lithologic Units III and IV below 180 mbsf (Fig. F2). Although backfill prevented logging of the volcanic basement, hole conditions remained stable long enough to log most of the sedimentary section within this interval of poor core recovery. The LSS, in the middle of the 33-m-long tool string, obtained velocity measurements from 160 (Subunit IIB) to 351 mbsf (Unit IV) ~59 m above the top of oceanic crust and 94 m above total hole depth (Fig. F3). A constant velocity (the average log velocity of lithologic Unit IV [2485 m/s]) was used to extend the log velocity from 351 mbsf down to the top of oceanic crust at 410 mbsf. The average laboratory-derived velocity of 4821 m/s was used to continue the velocity data from 410 to the total depth of 445.2 mbsf (Fig. F2).

Density values were acquired as shallow as 63 mbsf (Unit I) and extend down to 398 mbsf, ~12 m above the top of oceanic crust and 47 m above total hole depth (Fig. F3). A constant density, the average log density of the lowermost 50 m of lithologic Unit IV (2.2 g/cm^3), was used to extend the log density from 398 mbsf down to the top of oceanic crust at 410 mbsf. The average laboratory-derived density of 2.66 g/cm^3 was used to extend the density data to the total depth of 445.2 mbsf (Fig. F2). The combination of laboratory and downhole logging data used to make continuous velocity and density profiles are listed in Table T1.

T1. Depth intervals, hole designations, and measurement type for the velocity and density data, p. 14.

SYNTHETIC SEISMOGRAMS

Velocity and density data from laboratory and downhole measurements were converted from mbsf to two-way traveltime (TWT) and resampled at a 1-ms sample interval. Impedance (velocity × density) and impedance contrasts were used to calculate reflection coefficients (Fig. F2). This calculation is simplified by assuming vertical incidence, horizontal interfaces, no multiples, and no energy loss from spherical spreading and attenuation. The water gun seismic-source wavelet was obtained from the average of 10 adjacent traces of the seafloor reflection at the drill site. The portion of the stacked signal from the first negative to positive deflection associated with the seafloor to a point interpreted as the end of the source wavelet (31 ms) was used as the seismic source (Fig. F2). The series of reflection coefficients was convolved with the source wavelet to produce a minimum-phase synthetic seismogram. The merge point of laboratory and logging data at 180 mbsf occurs at a major change in lithology and physical properties (Unit II/III boundary) (Figs. F2, F3), and therefore, joining the data at that depth does not create an artificial impedance contrast. The use of a constant velocity in the lowermost 59 m of the sedimentary section, stepping to a higher constant velocity interval within the ~40 m of oceanic crust, only serves to model the TWT to the top of oceanic crust and not the seismic character (facies) of this short depth interval. The seismic character of this portion of the synthetic is controlled by the density log, which continues to 398 mbsf. An examination of the downhole resistivity and density measurements, which, like velocity, are largely controlled by porosity, indicate that there are no large reflection-producing changes in physical properties in the section immediately above basement (Fig. F3). More importantly, the length of the source wavelet is comparable to this depth interval and convolution with any reasonable velocity series covering this short 59-m interval will result in nearly identical synthetic seismograms with only the total traveltime changing.

RESULTS AND DISCUSSION

A synthetic seismogram can constrain depth–traveltime correlations if the synthetic seismogram closely matches the observed seismic character. Reflections, however, are most often interference patterns caused by the source wavelet character and combined impedance contrasts associated with closely spaced downhole changes in porosity and lithology. Exceptions include reflections created by large and abrupt impedance contrasts between extended intervals of relatively uniform physical properties where the reflection appears as a recognizable reproduction of the source wavelet scaled by the reflection coefficient (e.g., the seafloor). Reflections created at such interfaces are especially useful for constraining depth–traveltime correlations. Reflection amplitude is directly related to the size of the impedance contrast and can also be an important constraint when matching synthetic and observed seismograms. At Site 1149, a large contrast in physical properties at the interface between the thick (180 m) section of relatively homogenous pelagic clay and a sequence of interbedded chert/porcellanite/clay is expected to produce the shallowest subseafloor high-amplitude reflection (e.g., Wilkens et al., 1993).

Figure **F2** summarizes the core-log-seismic correlation at Site 1149 based on synthetic seismograms. The observed seismic data and synthetic seismogram are both displayed using identical parameters, including true relative amplitude, in order to clearly identify the highest amplitude events. A preliminary synthetic seismogram (not shown) matched all the major features of the observed seismic profile including the high-amplitude reflections expected from the largest impedance contrasts at the seafloor, the pelagic clay/chert interface (Unit II/III boundary), and the top of the oceanic crust. However, the TWT of the major subseafloor reflections on the preliminary synthetic seismogram were slightly larger (10 ms deeper) than those observed on seismic profiles. This indicates velocities used in this synthetic were slightly too low. The simplest solution to achieve a perfect match between the onset of the highest amplitude reflections of the synthetic and observed seismograms was to raise the average velocity (1525 m/s) of the laboratory-derived measurements in the upper 180 mbsf by 69 m/s, a 4.5% increase. Is this a valid solution? It is well known that laboratory measurements of velocity are lower than in situ measurements in unlithified marine sediments because of core expansion and disturbance created from the coring process. This indicates the sign of the correction is correct (i.e., laboratory velocities must increase), but is the amount of increase reasonable? The ~20-m interval (160–180 mbsf) of in situ velocity measurements overlapping with laboratory measurements in the pelagic clay (Subunit IIB) average of ~1568 m/s, a 3.5% increase over the average laboratory velocity in this interval. This result is very close to the amount of velocity increase required to exactly match synthetic and observed seismograms; however, downhole velocity measurements in this interval are extremely noisy because of widely varying borehole diameters and may be too low (Fig. **F3**).

Various site specific and general velocity vs. depth functions have been developed that correct laboratory velocities to reflect in situ conditions (e.g., Urmos et al., 1993; Carlson et al., 1986). Although these corrections are not specific to the high-porosity, high-clay content of Units I and II, they can serve as a general guide to in situ velocities in this short and shallow depth interval. Application of the corrections of either Urmos et al. (1993) or Carlson et al. (1986) to our data raises the average velocity in the 0–180 mbsf interval by ~7% (~1630 m/s) and places the first high-amplitude subseafloor reflection only 6 ms shallower than on the observed seismogram (i.e., decreases the TWT). Because the character of the observed seismic (i.e., both low and high amplitudes) is so well matched by the synthetic, the use of any of these corrections to laboratory velocities results in similar conclusions; the Unit II/III boundary at 180.12 mbsf corresponds to the shallowest subseafloor high-amplitude reflection at 226 milliseconds below seafloor (msbsf), and the top of oceanic crust at 410 mbsf corresponds to the high-amplitude reflection at 438 msbsf. The synthetic seismogram utilized in this paper applies the simplest solution of raising the laboratory velocities by a constant 69 m/s, resulting in an average velocity of 1594 m/s for the upper 180 m of sediment.

These results indicate that the correlation between lithologic unit boundaries (core depth) and TWT given by the Shipboard Scientific Party (2000c), which were established without the aid of synthetic seismograms, must be adjusted to slightly greater traveltimes. The Unit II/III boundary is placed at 226 msbsf rather than 200 msbsf. The Unit III/IV boundary correlates to 336 msbsf rather than 280 msbsf, and the top of oceanic crust is at 438 msbsf instead of 420 msbsf.

Seismic Stratigraphy

Ewing et al. (1968) originally defined the acoustic stratigraphy of large portions of the western Pacific as consisting of two or more of the following four seismic units: (1) an upper transparent layer (weakly reflective), (2) an upper opaque layer (highly reflective or well stratified), (3) a lower transparent layer, and (4) acoustic basement. Acoustic basement has been referred to as "Horizon B," the "deep opaque layer," and as the "reverberant layer" where it is characterized by an interval of flat-lying, smooth, high-amplitude, closely spaced reflections (Ewing et al., 1968; Heezen, MacGregor, et al., 1973; Houtz et al., 1973; Houtz and Ludwig, 1979).

These regional seismic facies are also apparent at Site 1149. The upper transparent layer is highlighted in brown, the upper opaque and lower transparent facies are shown in light blue, and acoustic basement is displayed in gray (Figs. F2, F4). The lowermost seismic facies, acoustic basement, is characterized by a single or two to three closely spaced high-amplitude continuous reflector(s) (Figs. F2, F4). These continuous reflections range in appearance from relatively smooth and flatlying to diffractive and undulating depending on seismic source and azimuth of profile direction. In Holes 1149A and 1149B, acoustic basement begins at 8138 milliseconds two-way traveltime (mstwt), equivalent to 438 msbsf, and is created from the impedance contrast between nannochalk/marl (Unit IV) and fractured basalt at 410 mbsf.

F4. SCS water gun lines 1, 2, and 3, p. 13.

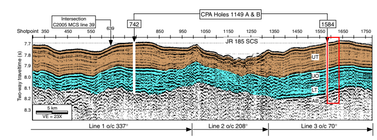

The lower transparent layer is poorly represented at Site 1149, and often, it appears that the upper opaque layer directly overlies oceanic crust, depending on processing parameters such as automatic gain control. The lower transparent facies appears as relatively low-amplitude discontinuous chaotic to hummocky reflections extending down to acoustic basement and exhibits pelagic sheet drape character because it is generally of uniform thickness and concordant with the underlying basement topography. This interval correlates to the interbedded chert/chalk/marl of lithologic Unit IV. The lithologic Unit III/IV boundary (282.9 mbsf = 336 msbsf), however, is not associated with a distinct continuous reflection because there is no large and abrupt impedance contrast at this boundary. Instead, it is characterized by a reflection interference pattern with a subtle transition from the upper opaque to the poorly developed lower transparent seismic facies.

The upper opaque layer as originally defined by analog air gun records appears stratified rather than "opaque" on these SCS water gun records (Figs. **F2, F4**). The upper opaque layer in Holes 1149A and 1149B begins at 226 msbsf (7926 mstwt) and consists of high-amplitude continuous reflections that mimic the underlying basement relief and appear as a stratified pelagic drape deposit of generally uniform thickness. The continuous high-amplitude reflection that appears at 226 msbsf is the result of the large and abrupt impedance contrast, which is present between pelagic clay (Unit II) and the shallowest abundant chert at ~180 mbsf (Unit III) (Figs. **F2, F4**). The stratified appearance is an interference pattern from closely spaced impedance contrasts associated with interbedded chert, porcellanite, and clay similar to that observed by Wilkens et al. (1993).

The upper transparent layer is relatively thick and extends from the seafloor to 226 msbsf (7926 mstwt). This unit has a pelagic sheet-drape form and a relatively reflection-free seismic character in the upper portion with semicontinuous reflections of low amplitude apparent in the lower portion of this interval. The "transparent" character is indicative of a relatively homogenous interval containing no significant impedance contrasts and is correlated to the unlithified siliceous ash-bearing clay of lithologic Subunit IA. The weak semicontinuous reflections beginning at 148 msbsf correlate to lithologic Unit II (118.2–180.12 mbsf). The Unit I/II boundary is marked by abrupt but relatively small changes in porosity, grain density, and downhole resistivity, and extreme changes in borehole diameter are present within Unit II (Fig. **F3**) (Shipboard Scientific Party, 2000c).

CONCLUSIONS

1. Correlations between core, logging, and seismic data from ODP Site 1149 have been established through the construction of a synthetic seismogram from a combination of downhole and shipboard laboratory measurements of velocity and density.
2. The major reflections and general seismic facies characteristics of the observed SCS profiles are well reproduced by the synthetic seismogram. The close match between synthetic and observed seismogram displayed using true amplitudes allows the synthetic to successfully constrain depth to traveltime correlations and requires that laboratory velocities be increased by ~4.5% in the upper transparent seismic facies. The velocity increase is consistent with results from other empirical methods that correct laboratory velocities for the effects of rebound and core disturbance.
3. The depth-to-traveltime correlations indicate that the lithologic unit boundaries given by the Shipboard Scientific Party (2000c) must be adjusted to slightly greater traveltimes as follows: Unit II/III boundary at 226 msbsf rather than 200 msbsf, Unit III/IV at

336 msbsf rather than 280 msbsf, and top of oceanic crust at 438 msbsf rather than 420 msbsf.

4. The seismic facies identified at Site 1149 can be compared to the regional seismic facies descriptions of the northwest Pacific by Ewing et al. (1968). No other boreholes within 1000 km of Site 1149 have sampled the complete sedimentary section and top of oceanic crust seaward of the Izu-Bonin trench. Thus, the results of the correlation between physical and seismic stratigraphy at Site 1149 have regional significance and can now be extended basinwide using preexisting regional MCS and analog SCS profiles.

ACKNOWLEDGMENTS

This research used samples and data provided by the Ocean Drilling Program (ODP). ODP is sponsored by the U.S. National Science Foundation and participating countries under the management of the Joint Oceanographic Institutions, Inc. This project was partially funded by the U.S. Science Support Program. This is University of North Carolina, Wilmington, Center for Marine Science Contribution #255.

I am grateful to the Ocean Drilling Program for inviting me to participate on Leg 185, to all members of the Shipboard Scientific Party of Leg 185 for their cooperation on board the ship, and to the ODP personnel and the SEDCO crew who made Leg 185 a success. I also thank Richard Jarrard for insights into the interpretation of shipboard physical properties data and Dr. Sun, at Lamont-Doherty Borehole Research Group, for supplying software for synthetic seismogram calculations. Maps were produced using Generic Mapping Tools software (Wessel and Smith, 1995). Reviews by William Sager and M.F. Moore improved this manuscript.

REFERENCES

Blum, P., 1997. Physical properties handbook: a guide to the shipboard measurement of physical properties of deep-sea cores. *ODP Tech. Note,* 26 [Online]. Available from World Wide Web: <http://www-odp.tamu.edu/publications/tnotes/tn26/INDEX.HTM>. [Cited 1999-04-01]

Boyce, R.E., 1976. Definitions and laboratory techniques of compressional sound velocity parameters and wet-water content, wet-bulk density, and porosity parameters by gravimetric and gamma-ray attenuation techniques. *In* Schlanger, S.O., Jackson, E.D., et al., *Init. Repts. DSDP,* 33: Washington (U.S. Govt. Printing Office), 931–958.

Carlson, R.L., Gangi, A.F., and Snow, K.R., 1986. Empirical reflection travel time versus depth and velocity versus depth functions for the deep sea sediment column. *J. Geophys. Res.,* 91:8249–8266.

Ewing, J., Ewing, M., Aitken, T., and Ludwig, W.J., 1968. North Pacific sediment layers measured by seismic profiling. *In* Knopoff, L., Drake, C.L., and Hart, P.J. (Eds.), *The Crust and Upper Mantle of the Pacific Area.* Geophys. Monogr., Am. Geophys. Union., 12:147–173.

Heezen, B.C., MacGregor, I.D., et al., 1973. *Init. Repts. DSDP,* 20: Washington (U.S. Govt. Printing Office).

Houtz, R.E., Ewing, J., and Buhl, P., 1970. Seismic data from sonobuoy stations in the northern and equatorial Pacific. *J. Geophys. Res.,* 75:5093–5111.

Houtz, R.E., and Ludwig, W.J., 1979. Distribution of reverberant subbottom layers in the southwest Pacific basin. *J. Geophys. Res.*, 84:3497–3504.

Smith, W.H.F., and Sandwell, D.T., 1997. Global seafloor topography from satellite altimetry and ship depth soundings. *Science,* 277:1956–1962.

Shipboard Scientific Party, 2000a. Explanatory notes. *In* Plank, T., Ludden, J.N., Escutia, C., et al., *Proc. ODP, Init. Repts.,* 185, 1–76 [CD-ROM]. Available from: Ocean Drilling Program, Texas A&M University, College Station TX 77845-9547, USA.

————, 2000b. Leg 185 summary: inputs to the Izu-Mariana subduction system. *In* Plank, T., Ludden, J.N., Escutia, C., et al., *Proc. ODP, Init. Repts.,* 185: College Station TX (Ocean Drilling Program), 1–63.

————, 2000c. Site 1149. *In* Plank, T., Ludden, J.N., Escutia, C., et al., *Proc. ODP, Init. Repts.,* 185, 1–190 [CD-ROM]. Available from: Ocean Drilling Program, Texas A&M University, College Station TX 77845-9547, USA.

Urmos, J., Wilkens, R.H., Bassinot, F., Lyle, M., Marsters, J.C., Mayer, L.A., and Mosher, D.C., 1993. Laboratory and well-log velocity and density measurements from the Ontong Java Plateau: new in-situ corrections to laboratory data for pelagic carbonates. *In* Berger, W.H., Kroenke, L.W., Mayer, L.A., et al., *Proc. ODP, Sci. Results,* 130: College Station, TX (Ocean Drilling Program), 607–622.

Wessel, P., and Smith, W.H.F., 1995. New version of the Generic Mapping Tools released. *Eos, Trans. Am. Geophys. Union,* 76:329.

Wilkens, R.H., Christensen, N.I., and Collins, J.A., 1993. Seismic properties and reflectivity of North Pacific Ocean cherts. *In* Wilkens, R.H., Firth, J., Bender, J., et al., *Proc. ODP, Sci. Results,* 136: College Station, TX (Ocean Drilling Program), 99–104.

Figure F1. A. Predicted topography of the northwest Pacific (Smith and Sandwell, 1997) and selected physiographic features. Circles locate Site 1149 (~100 km east of the Izu-Bonin Trench) and DSDP Sites 303 and 304. **B.** Circles indicate Site 1149 hole positions. The bold black line indicates the track of the ~50-km-long single-channel seismic (SCS) survey conducted during Leg 185 (*JOIDES Resolution*, Leg 185 SCS lines 1, 2, and 3). This SCS data is presented in Fig. **F4,** p. 13. The bold red line indicates the portion of SCS data displayed in Fig. **F2,** p. 11. The thin black line indicates a segment of multichannel seismic (MCS) line 39 from the regional survey of C2005.

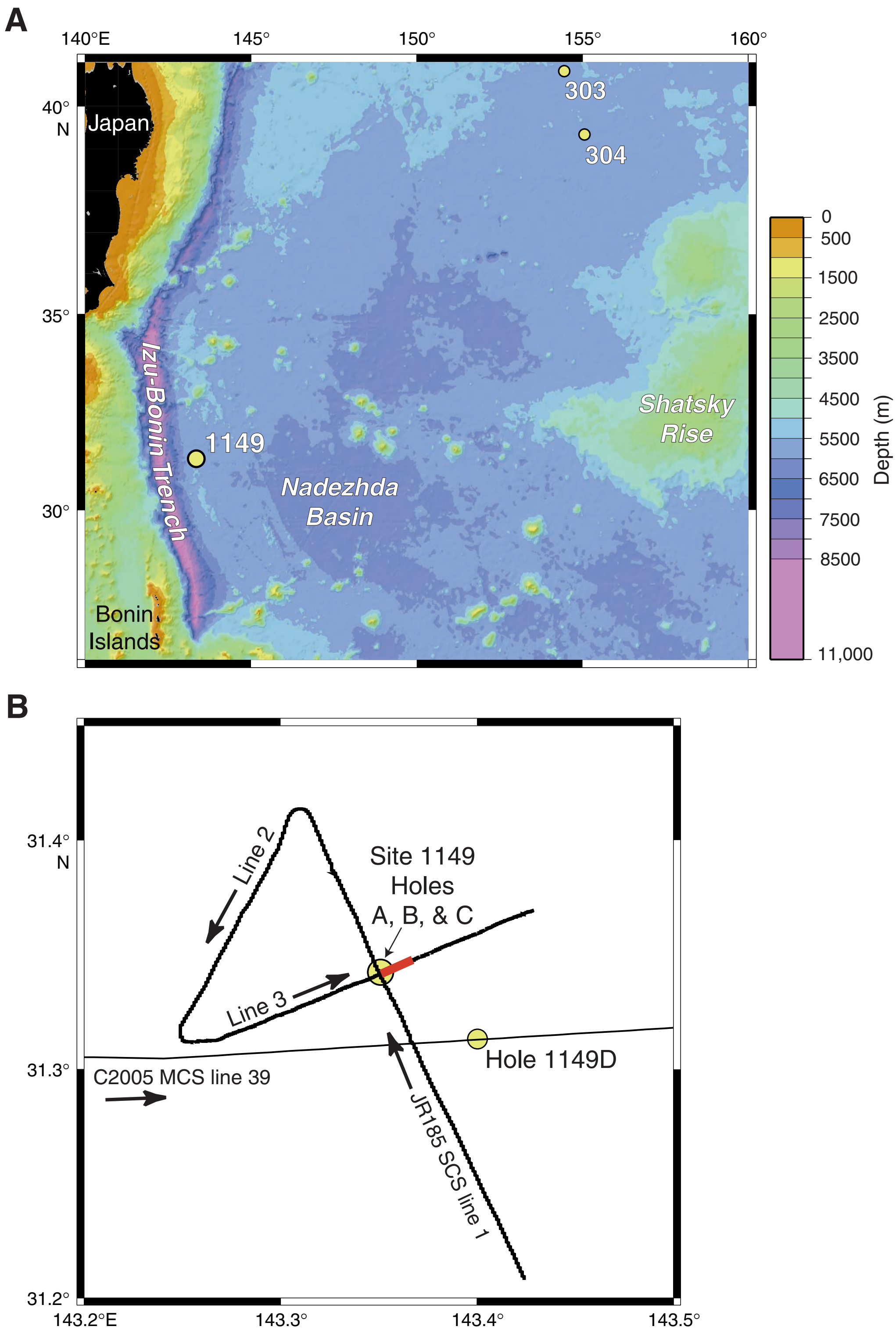

Figure F2. Logging and coring results (Shipboard Scientific Party, 2000c) and core-log-seismic correlation based on synthetic seismograms. The first two columns summarize the lithology, lithologic units, and biostratigraphic ages at Site 1149. Columns three and four show the velocity and density profiles derived from merging laboratory and downhole measurements. Column five shows the reflection coefficient calculated from impedance contrasts obtained from the composite velocity and density data. Columns six and seven show selected depth (mbsf) to time (msbsf) correlations from matching the synthetic and observed seismograms. The seismic source signature that is convolved with the reflection coefficient to create the synthetic seismogram (SYN) is shown at the top of column seven. The synthetic seismogram is presented as 10 adjacent traces in column eight. Column nine shows an ~1.8-km portion of *JOIDES Resolution* SCS water gun line 2. Synthetic and observed seismograms are displayed with no filtering and true amplitude. The locations of Holes 1149A and 1149B are shown with an arrow. Regionally identified seismic units are color coded as described in the text and Figure F4, p. 13. TD = total depth, TWT = two-way traveltime, msbsf = milliseconds below seafloor, V = velocity.

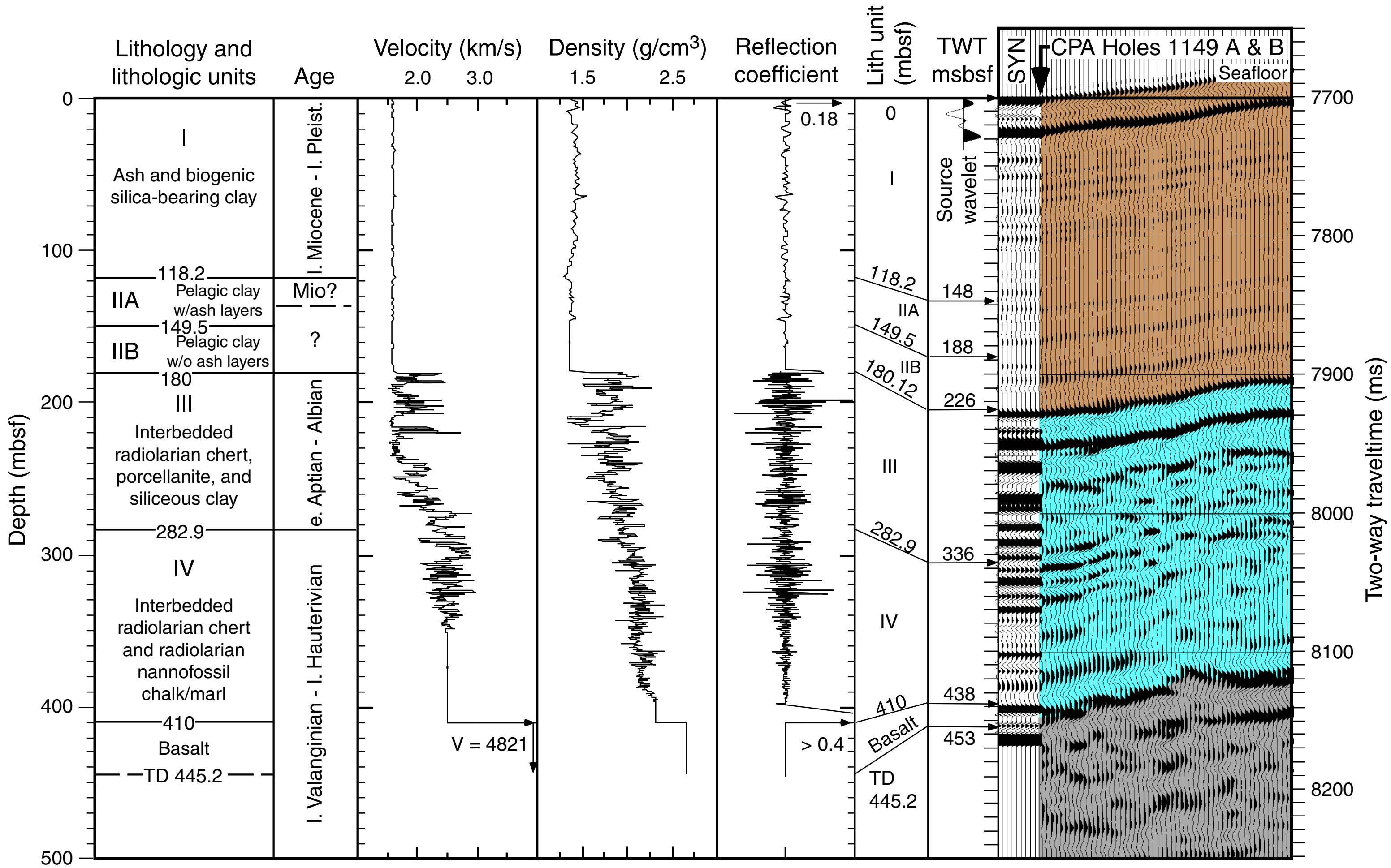

Figure F3. Lithology and lithologic units and downhole measurements of velocity, density, and resistivity (medium induction resistivity tool) along with the caliper from the HLDS tool are displayed through the entire logged section of Hole 1149B (Shipboard Scientific Party, 2000c). The dashed line highlights the abrupt and large contrast of physical properties at 180 mbsf. TD = total depth.

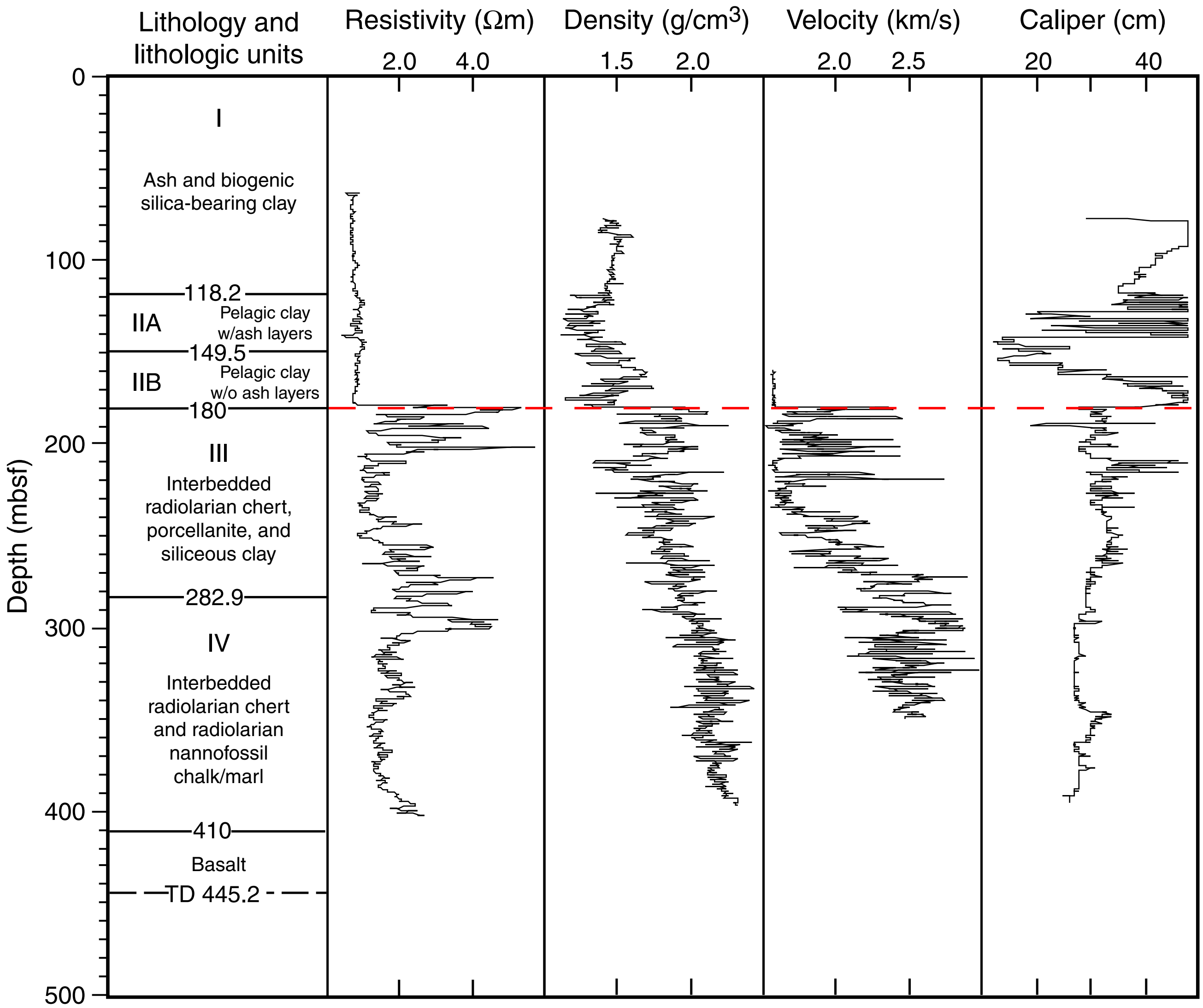

Figure F4. *JOIDES Resolution* (JR) single-channel seismic (SCS) water gun lines 1, 2, and 3. The bold white line at Shotpoints 742 and 1584 indicates the location and interval cored in Holes 1149A and 1149B. A box encloses the portion of SCS line 3 displayed in Figure F2, p. 11. Colors mark regionally identified seismic facies; light brown corresponds to the upper transparent layer (UT) and light blue encompasses the upper opaque (UO) and lower transparent (LT) layers lying above acoustic basement (AB). Seismic data were processed and displayed with the following parameters: seafloor mute, band-pass filter = 25–100 Hz, three-trace mix, plot every third trace, 500-ms AGC, and vertical exaggeration (VE) = 23× at the seafloor. MCS = multichannel seismic, CPA = closest point of approach, o/c = on course.

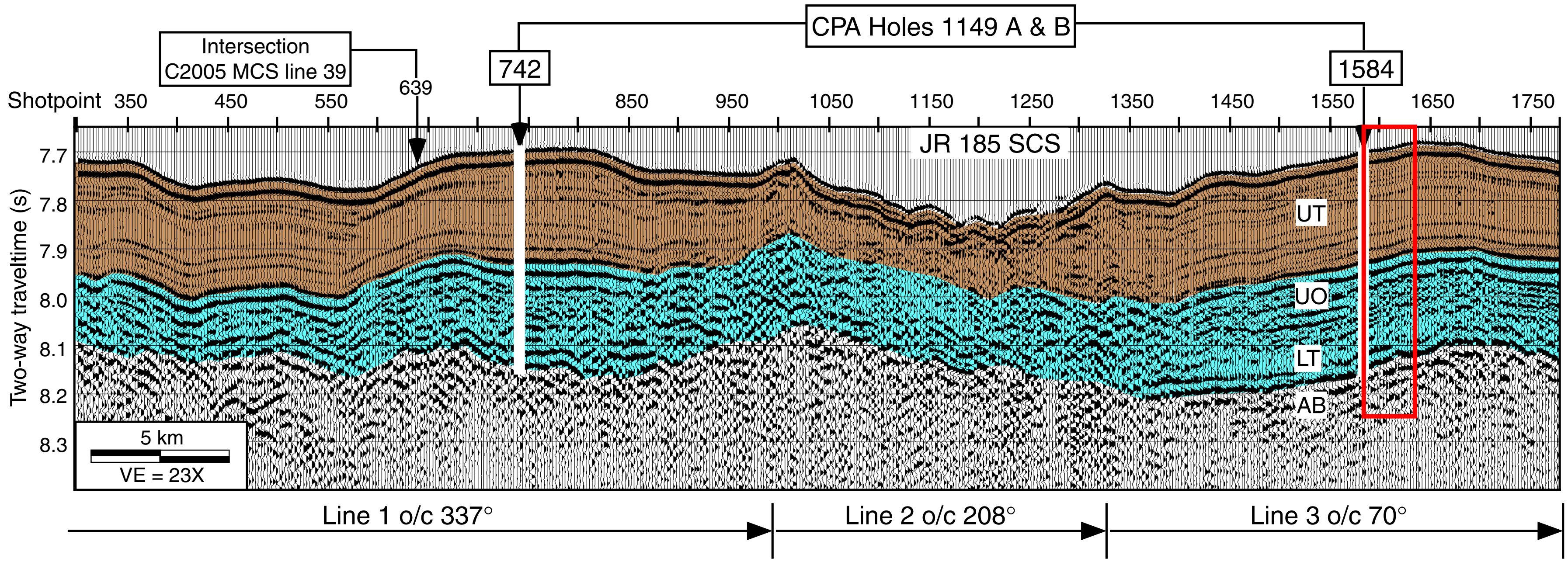

Table T1. Depth intervals, hole designation, and measurement type for the velocity and density data used to construct the synthetic seismogram (shown in Fig. F2, p. 11.).

Measurements	Velocity depth interval (mbsf)	Density depth interval (mbsf)
Shipboard laboratory	185-1149A, 185-1149B 0–179.55	185-1149A, 185-1149B 0–149 149–179.55 (use constant density of 1.36 g/cm^3)
	185-1149B 410–4145.2 (use average velocity of basalt = 4821 m/s)	185-1149B 410–445.2 (use average density of basalt = 2.66 g/cm^3)
Downhole (Hole 1149B)	180.12–350.83	180.12–397.9
	350.83–410.0 (use average velocity from 283 to 350.83 in lithologic Unit IV = 2485 m/s)	397.9–410.0 mbsf (use average density from 368 to 397.8 mbsf = 2.204 g/cm^3)